



Short communication

Development of a scalable spray pyrolysis process for the production of non-hollow battery materials



Miklos Lengyel ^a, Dror Elhassid ^b, Gal Atlas ^a, William T. Moller ^b, Richard L. Axelbaum ^{a,*}

^a Department of Energy, Environmental and Chemical Engineering, Washington University in St. Louis, One Brookings Drive, St. Louis, MO 63130, USA

^b X-Tend Energy LLC, 1005 North Warson Road, St. Louis, MO 63132 USA

HIGHLIGHTS

- A novel slurry spray pyrolysis process is reported.
- 5–7 μm particles with a solid interior morphology are produced.
- Production rates exceed 50 g h^{-1} .
- Tap density of product is greater than 1 g cm^{-3} .
- $\text{Li}_{1.2}\text{Mn}_{0.54}\text{Ni}_{0.13}\text{Co}_{0.13}\text{O}_2$ demonstrates excellent electrochemical performance.

ARTICLE INFO

Article history:

Received 5 March 2014

Received in revised form

29 April 2014

Accepted 29 April 2014

Available online 9 May 2014

Keywords:

Spray pyrolysis

Flame assisted spray pyrolysis

Lithium ion batteries

Scale up

Non-hollow spheres

ABSTRACT

Spray pyrolysis typically produces hollow particles when the particles are larger than about 2 microns. In this work, a scalable spray pyrolysis process was developed for the production of electrochemically active materials in a way that overcomes hollow sphere formation. With this new slurry spray pyrolysis process particles greater than 6 μm have been successfully produced with a solid, yet porous interior morphology. Results indicate that the process shows great potential for the production of high quality, electrochemically active materials, as demonstrated by the electrochemical performance of layered $\text{Li}_{1.2}\text{Mn}_{0.54}\text{Ni}_{0.13}\text{Co}_{0.13}\text{O}_2$ materials. The materials are phase pure, as observed by powder X-ray diffraction (XRD), and discharge capacities greater than 200 mAh g^{-1} after 100 cycles at C/3 rate (where 1 C = 200 mAh g^{-1}) are consistently obtained. The standard deviation in discharge capacity for 5 batches of material produced under identical conditions was 11 mAh g^{-1} . These promising electrochemical results were obtained at a scale of 50 g h^{-1} and with minimal process optimization, indicating the potential for commercial scale production.

© 2014 Elsevier B.V. All rights reserved.

1. Introduction

To attain high quality low-cost batteries, inexpensive, scalable and highly reproducible processes are needed for synthesizing electrochemically active materials. Conventional synthesis methods for battery materials include sol–gel processes, solid-state synthesis and co-precipitation [1–4]. Co-precipitation can deliver materials with excellent electrochemical performance and high tap density ($>1.0 \text{ g cm}^{-3}$) at a laboratory scale. Yet, the process presents challenges in terms of scale up, including long processing times during precipitation (up to 24 h), extended

annealing conditions because of post-lithiation ($>5\text{--}20 \text{ h}$ at 900–1000 °C), excessive waste products due to several purification steps, and issues related to product uniformity and reproducibility.

Recently, spray pyrolysis has been developed for the production of layered cathode materials and the materials have shown excellent electrochemical performance, comparable to or exceeding that of materials produced by co-precipitation [5,6]. Spray pyrolysis is a fast and inexpensive method of producing multicomponent oxides, including lithium ion battery cathode materials [7–9]. The process is robust and delivers uniform materials due to the one droplet – one particle conversion mechanism. The main process variables can also be controlled accurately [10]. Typical process times in the reactor are on the order of a few seconds, and a post heat treatment at 800–900 °C for 2 h is typically sufficient to obtain the desired

* Corresponding author. Tel.: +1 314 935 7560; fax: +1 314 935 5464.

E-mail address: axelbaum@wustl.edu (R.L. Axelbaum).

crystallinity and electrochemical performance. This offers significant cost advantages compared to other synthesis methods, and the materials display excellent reproducibility. A recent study by Oljaca and coworkers from Cabot Corp. offered a comprehensive comparison of materials synthesized via spray pyrolysis and coprecipitation, demonstrating distinct advantages for spray pyrolysis [11]. Despite the advantages of spray pyrolysis, hollow and deformed spheres are typically produced when the secondary particles are larger than approximately 2 μm . These particles form from the larger droplets and are hollow due to the rapid surface precipitation and melt formation encountered in the process [8,12,13]. If hollow spheres can be eliminated, spray pyrolysis offers significant advantages over other synthesis processes in terms of process and equipment costs.

This paper presents an approach to avoid hollow sphere formation in a scalable process via a flame-assisted slurry spray pyrolysis process. The process is termed Flame Assisted Spray Technology-Slurry Spray Pyrolysis (FAST-SSP). Herein we report on the process and the electrochemical properties of $\text{Li}_{1.2}\text{Mn}_{0.54}\text{Ni}_{0.13}\text{Co}_{0.13}\text{O}_2$ synthesized via FAST – SSP.

2. Experimental

Fig. 1a shows the steps of the FAST – SSP process. First, the precursor solution is employed in conventional spray pyrolysis to form particles of the desired material. These materials are then milled to break-up hollow spheres and the powder is converted into a slurry with a precursor solution that has the same composition as the original precursor solution. This slurry becomes the precursor for subsequent spray pyrolysis.

The spray pyrolysis experimental setup is displayed in **Fig. 1b** [5,14]. The system, termed Flame Assisted Spray Technology (FAST), incorporates a back flame for heating, and a two-fluid nozzle (Delavan Inc.) to generate the spray. The feed rate of the nozzle is adjusted to produce materials at $>50 \text{ g h}^{-1}$. The typical residence time in the system is about 1 s and the temperature at the exit of the reactor is approximately 500–600 $^{\circ}\text{C}$.

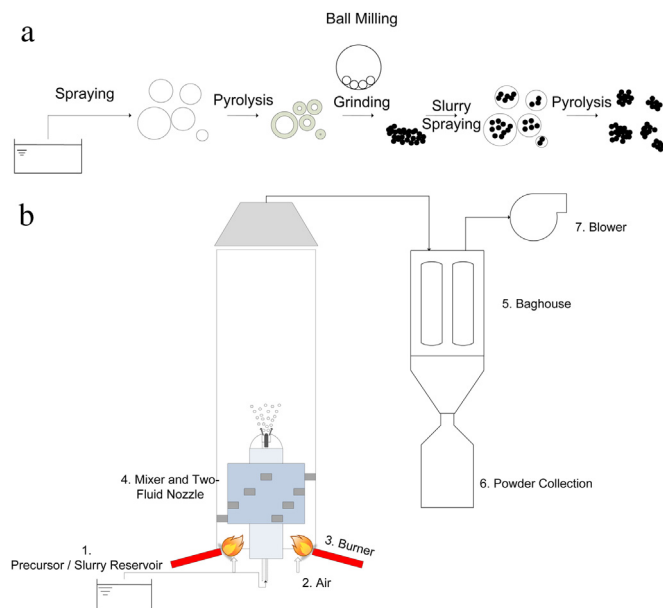


Fig. 1. (a) Block flow diagram of the FAST-SSP process; and (b) schematic diagram of the FAST-SSP setup. (1) Precursor/slurry reservoir; (2) excess air supply; (3) burners; (4) mixer and two-fluid nozzle; (5) baghouse filter; (6) powder collection; and (7) blower.

The precursor solution was prepared by dissolving LiNO_3 , $\text{Mn}(\text{NO}_3)_2 \cdot 4\text{H}_2\text{O}$, $\text{Ni}(\text{NO}_3)_2 \cdot 6\text{H}_2\text{O}$ and $\text{Co}(\text{NO}_3)_2 \cdot 6\text{H}_2\text{O}$ (Alfa Aesar) in deionized water at the precursor ratio corresponding to the chemistry for $\text{Li}_{1.2}\text{Mn}_{0.54}\text{Ni}_{0.13}\text{Co}_{0.13}\text{O}_2$. The total dissolved salt concentration was fixed at 2.5 mol L^{-1} (M).

The as-synthesized samples after FAST-SSP were subject to an annealing heat treatment at 900 $^{\circ}\text{C}$ for 2 h. The annealed powders were characterized by XRD using a Rigaku Diffractometer (Geigerflex D-MAX/A) at a scan rate of 0.04 $^{\circ}$ s^{-1} between 10 $^{\circ}$ and 80 $^{\circ}$ 2Θ . The tapped powder density of the material was measured by a Quantachrome Autotap tapped density analyzer. Particle morphology was examined with an FEI Nova 2300 Field Emission SEM. The interior morphology of the product powder was observed by embedding the powder in an epoxy-based resin. Two μm thick sections were cut by a Leica Ultramicrotome and the sections were examined by SEM microscopy.

Cathode film fabrication was performed according to the procedure reported earlier [5]. The cathode slurry was prepared using 10 wt% polyvinylidene fluoride (PVdF) binder solution (Kureha Corp. Japan), 10 wt% Super-C45 conductive carbon black (Timcal) suspended in 1-methyl-2-pyrrolidinone (NMP–Sigma Aldrich) and 80 wt% active material. The active material loading density was between 2.5 and 4.0 mg cm^{-2} . Half-cells were assembled for the electrochemical tests using pure lithium anodes and 2500 Celgard membranes (Celgard, LLC). The electrolyte solution was 1.2 M LiPF_6

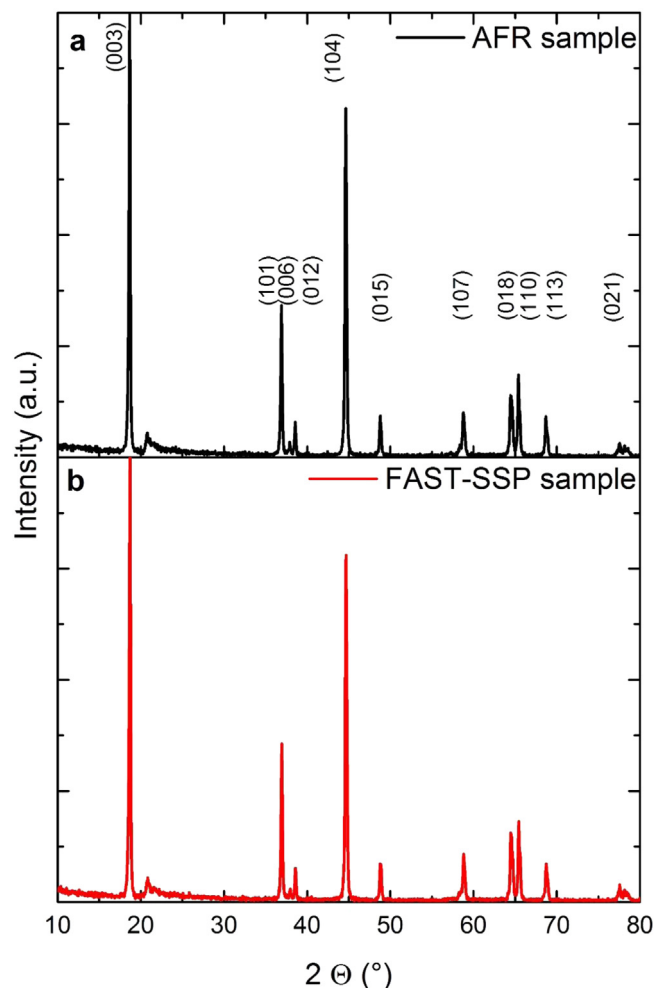


Fig. 2. Comparison of the XRD patterns from $\text{Li}_{1.2}\text{Mn}_{0.54}\text{Ni}_{0.13}\text{Co}_{0.13}\text{O}_2$ powders synthesized via (a) AFR and (b) FAST-SSP.

in ethylene carbonate/ethyl-methyl-carbonate solution (EC:EMC = 3:7 by weight) (Tomiyama High Purity Chemicals). The cells were activated between 2.0 and 4.8 V at 20 mA g⁻¹ (C/10) and then cycled between 2.0 and 4.6 V at 20 mA g⁻¹ and then 66.7 mA g⁻¹ (C/3). Rate capability tests ranged between 20 mA g⁻¹ (C/10) and 200 mA g⁻¹ (C/1) according to the protocols reported earlier [10].

The electrochemical performance of the powders was evaluated in 2032-type coin cells (Hohsen Corporation) assembled in an argon-filled glove box. Cycling tests were performed using an MTI-BST8-WA-type battery tester. The electrochemical tests were performed at 22 °C.

3. Results and discussion

3.1. Material characterization

In Fig. 2 the XRD patterns for the Li_{1.2}Mn_{0.54}Ni_{0.13}Co_{0.13}O₂ cathode materials synthesized using the FAST-SSP are compared with the same material synthesized using a standard Aerosol Flow Reactor (AFR) [15]. Most of the diffraction peaks can be indexed according to the α -NaFeO₂ (R-3m) structure. The splitting of the (006), (012) and (018), (110) peaks indicate a layered structure. The broad peak between 20 and 25° 2θ is characteristic of the super-lattice ordering between the LiMn_{0.33}Ni_{0.33}Co_{0.33}O₂ and the Li₂MnO₃ components that form the layered composite cathodes [16]. Clearly, no significant difference can be observed in the XRD pattern of the materials synthesized by the two methods, despite the fact that the production rates of the FAST-SSP system are 50 times greater than that of the AFR system.

The typical morphology of particles produced from the AFR is spherical provided that the particles are less than 2 microns [5]. Larger particles can be deformed due to their hollow interior, as shown in Fig. 3a. Fig. 3b shows the microtome of the particles produced by spray pyrolysis and the hollow interior is clearly visible.

Fig. 3c shows the morphology of the particles synthesized via FAST-SSP. The secondary particles are non-spherical and display a relatively wide size distribution ranging from 1 to 10 μm, with a mean particle size between 4 and 5 μm. The primary particle size is between 200 and 400 nm. The interior morphology of the particles is shown in Fig. 3d. These results show significant improvements in morphology compared to materials synthesized via ultrasonic spray pyrolysis [10]. Due to the slurry spraying step the interior morphology of larger particles is either solid (and porous) or the interior hollowness is significantly reduced. Particles above 6 μm in size with a solid (non-hollow) interior morphology can be clearly observed. To the best knowledge of the authors these are the largest non-hollow particles synthesized via spray pyrolysis. The tapped powder density of the material after FAST-SSP was found to be 1.05 g cm⁻³ compared to 0.4–0.6 g cm⁻³ obtained by ultrasonic spray pyrolysis [10]. The non-hollow morphology is clearly responsible for the improvement in the tapped density of the material.

Fig. 4 compares the cycle and rate capability test results for materials synthesized via FAST-SSP with those via the AFR. These results indicate that the electrochemical performance of the materials synthesized via FAST-SSP are excellent, similar to those obtained when synthesized via the AFR or co-precipitation [17]. The reproducibility of the process was evaluated by synthesizing five

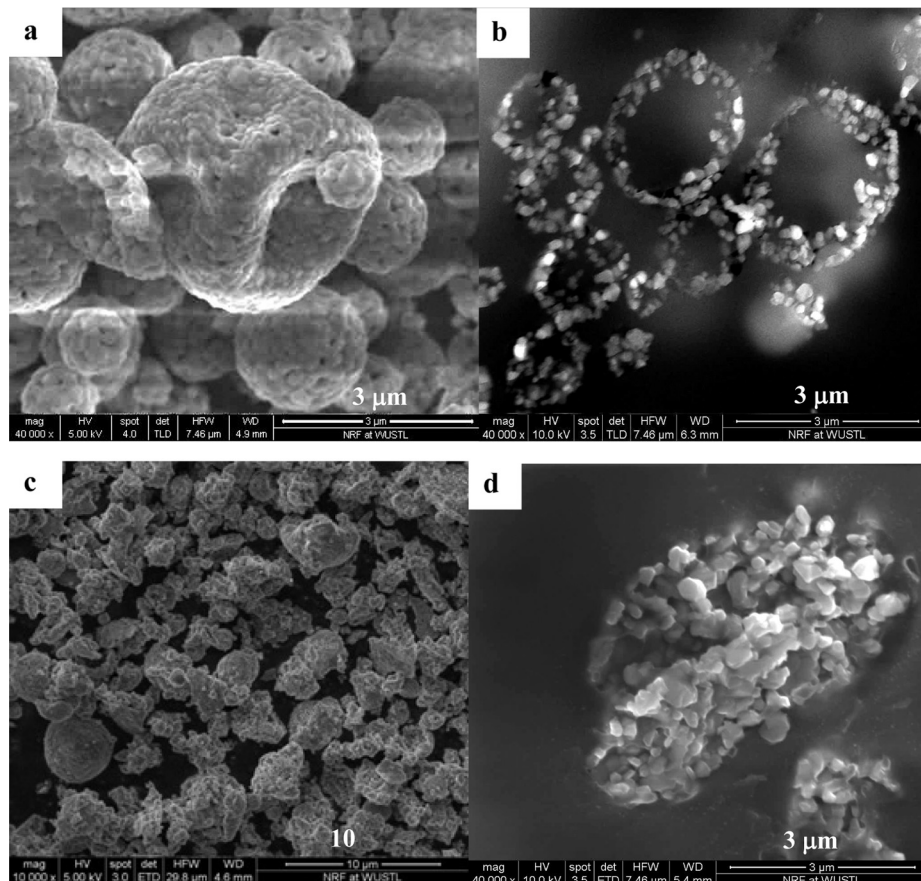


Fig. 3. Morphology of Li_{1.2}Mn_{0.54}Ni_{0.13}Co_{0.13}O₂ synthesized via (a) AFR; (b) interior structure after AFR synthesis; (c) FAST-SSP; (d) interior structure after FAST-SSP, as observed by SEM.

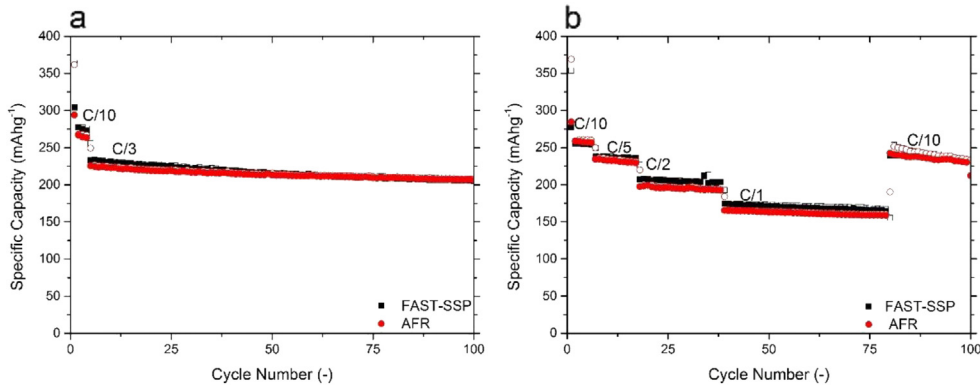


Fig. 4. Comparison of (a) cycling and (b) rate capability of $\text{Li}_{1.2}\text{Mn}_{0.54}\text{Ni}_{0.13}\text{Co}_{0.13}\text{O}_2$ powders synthesized via AFR and FAST-SSP.

batches of $\text{Li}_{1.2}\text{Mn}_{0.54}\text{Ni}_{0.13}\text{Co}_{0.13}\text{O}_2$ under identical synthesis conditions on five different days. The electrochemical performance was evaluated for each batch in cycle tests and the standard deviation of the discharge capacities at C/3 rate was $\sim 11 \text{ mAh g}^{-1}$. Fig. 4a shows that after 100 cycles at C/3 rate the discharge capacity exceeds 200 mAh g^{-1} . Rate capability tests indicate discharge capacities $>170 \text{ mAh g}^{-1}$ at 1 C rate. No irreversible capacity loss was observed during the rate capability tests. It is clear that improvements in production rate, morphology and tapped density can be achieved without compromising the electrochemical performance of the material.

4. Conclusions

A novel slurry spray pyrolysis process (FAST-SSP) was demonstrated by synthesizing powders of the layered $\text{Li}_{1.2}\text{Mn}_{0.54}\text{Ni}_{0.13}\text{Co}_{0.13}\text{O}_2$ material. The process shows high potential for large scale synthesis of cathode materials and yields improved tapped density compared to traditional spray pyrolysis. For the layered materials the tapped density increased from 0.4 g cm^{-3} to greater than 1.0 g cm^{-3} . FAST-SSP is the only known solution for addressing the hollow spheres during spray pyrolysis.

The electrochemical results for $\text{Li}_{1.2}\text{Mn}_{0.54}\text{Ni}_{0.13}\text{Co}_{0.13}\text{O}_2$ powders indicate that performance comparable to that obtained either via traditional spray pyrolysis or co-precipitation can be obtained via FAST-SSP. FAST-SSP is a simple, scalable, rapid process that yields excellent reproducibility and offers significant potential for reducing processing and production costs of cathode materials, suggesting high potential for commercial scale production.

Acknowledgements

The authors are grateful to the NSF for support under Grant No. 0928964 and to X-tend Energy LLC (NSF Award # CBET-0928964). The authors are grateful to Howard Wynder for his help in the preparation of the microtome cross sections. This work was also

supported by the Nano Research Facility (NRF), a member of the National Nanotechnology Infrastructure Network (NNIN), which is supported by the National Science Foundation under Grant No. ECS-0335765. Any opinions, findings, conclusions, or recommendations expressed in this material are those of the author(s) and do not necessarily reflect the views of the National Science Foundation. NRF is part of the School of Engineering and Applied Science at Washington University in St. Louis. RLA and Washington University may receive income based on a license of related technology by the University to X-tend Energy LLC.

References

- [1] C.S. Johnson, J.-S. Kim, C. Lefief, N. Li, J.T. Vaughan, M.M. Thackeray, *Electrochim. Commun.* 6 (2004) 1085–1091.
- [2] Z. Lu, D.D. MacNeil, J.R. Dahn, *Electrochim. Solid State Lett.* 4 (2001) A191–A194.
- [3] J.W. Fergus, *J. Power Sources* 195 (2010) 939–954.
- [4] N. Yabuuchi, K. Yoshii, S.-T. Myung, I. Nakai, S. Komaba, *J. Am. Chem. Soc.* 133 (2011) 4404–4419.
- [5] X. Zhang, R.L. Axelbaum, *J. Electrochem. Soc.* 159 (2012) A834–A842.
- [6] X. Zhang, M. Lengyel, R.L. Axelbaum, *AIChE J.* 60 (2014) 443–450.
- [7] M.Y. Son, Y.J. Hong, S.H. Choi, Y.C. Kang, *Electrochim. Acta* 103 (2013) 110–118.
- [8] G.L. Messing, S.C. Zhang, G.V. Jayanthi, *J. Am. Ceram. Soc.* 76 (1993) 2707–2726.
- [9] S.H. Park, C.S. Yoon, S.G. Kang, H.-S. Kim, S.-I. Moon, Y.-K. Sun, *Electrochim. Acta* 49 (2004) 557–563.
- [10] M. Lengyel, G. Atlas, D. Elhassid, P.Y. Luo, X. Zhang, I. Belharouak, R.L. Axelbaum, *J. Power Sources* 262 (2014) 286–296.
- [11] M. Olijaca, B. Blizanac, A.D. Pasquier, Y. Sun, R. Bontchev, A. Suszko, R. Wall, K. Koehlert, *J. Power Sources* 248 (2014) 729–738.
- [12] M. Yamada, B. Dongying, T. Kodera, K. Myoujin, T. Ogihara, *J. Ceram. Soc. Jpn.* 117 (2009) 1017–1020.
- [13] S. Jain, D.J. Skamser, T.T. Kudas, *Aerosol Sci. Technol.* 27 (1997) 575–590.
- [14] X. Zhang, H. Zheng, V. Battaglia, R.L. Axelbaum, *J. Power Sources* 196 (2011) 3640–3645.
- [15] M. Lengyel, X. Zhang, G. Atlas, H.L. Bretscher, I. Belharouak, R.L. Axelbaum, *J. Electrochem. Soc.* (2014) in press.
- [16] Y. Li, M. Bettge, B. Polzin, Y. Zhu, M. Balasubramanian, D.P. Abraham, *J. Electrochem. Soc.* 160 (2013) A3006–A3019.
- [17] H. Deng, I. Belharouak, H. Wu, D. Dambournet, K. Amine, *J. Electrochem. Soc.* 157 (2010) A776–A781.